

# Suppression of Centromere Dynamics by Taxol® in Living Osteosarcoma Cells<sup>1</sup>

Jonathan Kelling, Kevin Sullivan, Leslie Wilson, and Mary Ann Jordan<sup>2</sup>

Department of Molecular, Cellular, and Developmental Biology and the Neuroscience Research Institute, University of California Santa Barbara, Santa Barbara, California 93106 [J. K., L. W., M. A. J.], and Department of Cell Biology, Scripps Research Institute, La Jolla, California 92037 [K. S.]

## ABSTRACT

Taxol® potently blocks mitosis at the transition from metaphase to anaphase, leading to apoptosis in many types of tumor cells. However, the precise mechanism of action of Taxol® is not understood. Here we have tested the hypothesis that a primary mechanism of action of Taxol® involves suppression of spindle microtubule dynamics. We have used centromere-binding protein B coupled to green fluorescent protein as a marker for the kinetochores and centromeres of chromosomes and analyzed the effects of low Taxol® concentrations on the dynamics of centromeres during metaphase of mitosis in living human osteosarcoma (U2OS) cells by quantitative time-lapse confocal microscopy. In the absence of Taxol®, the centromere pairs on attached sister chromatids alternately stretch apart and relax back together approximately 1.2 times/min due to tension on the kinetochores produced by the spindle microtubules (referred to here as centromere dynamics). We found that 50–100 nM Taxol® significantly suppressed centromere dynamics. For example, Taxol® reduced the mean separation distance between the sister centromeres from 0.73 to 0.65  $\mu\text{m}$ , a distance equivalent to that observed in the complete absence of microtubules. The frequency of transitions between stretching and relaxing was also significantly diminished by Taxol® (by 27%–35%). The suppressive effects of Taxol® on centromere dynamics were associated with maximal accumulation of cells at mitosis (63%), a >90% block of the metaphase/anaphase transition, and complete inhibition of cell proliferation. The data strongly support the idea that the inhibition of centromere dynamics by Taxol® prevents silencing of the mitotic spindle surveillance (checkpoint) mechanism. Because Taxol® strongly suppresses microtubule dynamics, the data also indicate that centromere dynamics can be accounted for by microtubule dynamics and may not require significant energetic contributions from microtubule motors. The strict correlation between the degree of suppression of centromere dynamics by Taxol® and the degree of mitotic block strongly indicates that the primary mechanism responsible for the mitotic block by Taxol® in U2OS cells involves suppression of the polymerization dynamics of kinetochore microtubules.

## INTRODUCTION

Taxol® is an important cancer chemotherapeutic agent that is effective for the treatment of many types of cancer (1). At high concentrations, Taxol® enhances microtubule polymerization and stabilizes microtubules against depolymerization (2–4), whereas at low concentrations, Taxol® strongly suppresses microtubule dynamic instability preferentially at microtubule plus ends along with only a modest increase in microtubule polymer mass (5–7). In many cells, Taxol® blocks mitosis at the transition from metaphase to anaphase (5, 8), leading ultimately to apoptosis (9, 10). The effects of Taxol® on mitosis appear due to an action on the spindle microtubules; however, the precise mechanism of action of Taxol® is not understood.

Microtubules are intrinsically dynamic polymers that undergo two kinds of dynamic behavior, “dynamic instability” and “treadmilling.” Dynamic instability is the stochastic switching of microtubule ends

between episodes of prolonged growing and rapid shortening (11). Treadmilling consists of net growing at microtubule plus ends and net shortening at minus ends (12, 13). Both extensive dynamic instability and treadmilling (or flux) occur in mitotic spindles, and the rapid dynamics of spindle microtubules play a critical role in the intricate movements of the chromosomes (8, 14–16). Low concentrations of Taxol® potently suppress microtubule growth and shortening in human cells during interphase at concentrations that inhibit proliferation of the cells and block mitosis (17, 18). This observation has led us to hypothesize that suppression of spindle microtubule dynamics by Taxol® is responsible for its potent ability to inhibit mitotic progression and cell proliferation. However, it has not been possible to visualize the dynamics of individual microtubules attached to chromosomes (the “kinetochore microtubules”) in the central spindle of living cells because the microtubule density is too great. Thus we sought a novel method to analyze the effects of Taxol® on kinetochore microtubule dynamics and directly test the hypothesis that suppression of spindle microtubule dynamics is responsible for mitotic block.

During metaphase of mitosis, the duplicated chromosomes with their kinetochore-attached microtubules are aligned at the metaphase plate and oscillate toward and away from the spindle poles (19). The centromeres of sister chromatids also repeatedly separate from each other (they stretch apart) and then return to a relaxed position [referred to here as centromere dynamics (20)]. Elastic heterochromatin lies between the sister centromeres; it is rich in  $\alpha$ -satellite DNA and contains proteins that are involved in maintaining sister chromatid cohesion. The kinetochores containing the plus ends of microtubules embedded in them lie adjacent to the centromeres, and it is the dynamic kinetochore microtubules that appear responsible for centromere dynamics.

In the present study, we used GFP<sup>3</sup>-labeled CENP-B (GFP-CENP-B), a centromere-binding protein, to examine the effects of Taxol® on the centromere dynamics in human osteosarcoma (U2OS) cells during metaphase of mitosis. We found that Taxol® (50–100 nM) suppressed the rates of stretching and relaxing of sister centromere pairs and significantly decreased the separation distance between the centromeres. The same concentrations of Taxol® that suppressed centromere dynamics also blocked mitosis, preventing progression from metaphase to anaphase. Together, these observations strongly support the hypothesis that the mechanism by which Taxol® inhibits mitosis and cell cycle progression into anaphase in U2OS cells is suppression of spindle microtubule dynamics.

## MATERIALS AND METHODS

**Cell Culture.** U2OS human osteosarcoma cells (American Type Culture Collection HTB96) were maintained in DMEM with 1% penicillin-streptomycin (Sigma, St. Louis, MO) and 10% fetal bovine serum (Atlanta Biologicals, Norcross, GA) at 37°C in a 5% CO<sub>2</sub> atmosphere; doubling time was 28 h. Cells were transfected with a CENP-B-GFP plasmid (20). Expression of GFP-CENP-B was stable for 2–6 weeks; cells were periodically reselected with 1.2  $\mu\text{g}/\text{ml}$  G418 to maintain maximal GFP signal.

<sup>3</sup> The abbreviations used are: GFP, green fluorescent protein; CENP-B, centromere-binding protein B.

Received 10/21/02; accepted 4/2/03.

The costs of publication of this article were defrayed in part by the payment of page charges. This article must therefore be hereby marked *advertisement* in accordance with 18 U.S.C. Section 1734 solely to indicate this fact.

<sup>1</sup> Supported by NIH Grants CA 57291 (to M. A. J. and L. W.) and GM39068 (to K. S.).

<sup>2</sup> To whom requests for reprints should be addressed. Phone: (805) 893-5317; Fax: (805) 893-4724; E-mail: jordan@lifesci.ucsb.edu.

**Immunofluorescence Microscopy.** Localization of microtubules and chromosomes was performed on cells that were fixed in 10% formalin in PBS (20 min, 25°C) followed by 10 min in methanol (4°C), washed with PBS containing 1% BSA, and incubated with rabbit anti- $\alpha$ -tubulin (DM1a; Sigma) and mouse antihuman histone monoclonal antibody (or 4',6-diamidino-2-phenylindole) to stain nuclei and chromosomes followed by incubation with a goat antirabbit rhodamine-conjugated secondary antibody and CY5-conjugated antimurine antibody (Jackson ImmunoResearch, West Grove, PA). Images were captured with a Bio-Rad MRC 1024 (Bio-Rad Laboratories, Hercules, CA) confocal microscope with an argon ion laser scanning head at 10% laser power, mounted on a Nikon Diaphot 200 inverted microscope, or with a Nikon Eclipse fluorescence microscope, using  $63 \times 1.4\text{NA}$  PlanApo lenses.

**Cell Proliferation and Mitotic Index.** Cells were seeded in 6-well plates (Falcon; Becton Dickinson, Lincoln Park, NJ) at  $8 \times 10^4$  cells/well. One to two days later, media were replaced with fresh media containing a range of Taxol® concentrations (5 nM to 1  $\mu\text{M}$ ) and further incubated for one cell cycle (28 h). The numbers of cells before and after incubation with Taxol® were determined by combining floating cells with attached cells (released by trypsinization for 10 min, 37°C) and then counting cells by using a hemacytometer. Mitotic index was determined by microscopic examination of chromosomes and GFP-CENP-B centromeres in cells that were collected as described above, fixed in formalin/methanol, stained with 4',6-diamidino-2-phenylindole, and imaged as described above. Results are the mean  $\pm$  SE of three independent experiments, with a minimum of 1000 cells counted for each condition in each experiment.

**Determination of Anaphase:Metaphase Ratio.** The ratio of the number of cells in anaphase to the number of cells in metaphase was determined by examining centromere arrangement in living cells by confocal microscopy of GFP-CENP-B for at least 50 cells in metaphase and anaphase as described further below. Results are the mean  $\pm$  SE of three independent experiments.

**Imaging of Centromeres in Living Cells.** After incubation with Taxol® for 6 h to allow attainment of an equilibrium drug concentration in the cells (21), polylysine-coated coverslips with live cells attached were mounted in a Dvorak-Stotler chamber (Nicholson Precision Instruments, Gaithersburg, MD) in the medium in which they had been cultured (with or without Taxol®) and maintained on the microscope stage at 35°C to 37°C by means of an air curtain incubator or an enclosed thermostat-regulated warmed lucite chamber. Images of live cells were collected on a Bio-Rad MRC 1024 confocal microscope mounted on a Zeiss Axiovert 100 inverted microscope using a  $63 \times 1.4\text{NA}$  Zeiss Neo Fluor lens with a 7.16 zoom at 3% laser power or on a Nikon Diaphot 200 microscope (described above). Pairs of fluorescent centromeres in mitosis orient perpendicular to the Z axis of the microscope and thus were easily identified. Each time course consisted of a series of 120 single images (4 Kalman averages each) at 5-s intervals (total time, 10 min) collected in a focal plane with an optical depth of 0.5  $\mu\text{m}$ . In each time course, several centromere pairs could be distinguished and followed.

**Image Processing and Quantitative Motility Analysis.** Time-lapse image sequences were viewed as movies using Bio-Rad Confocal Assistant Software 4.01 to identify centromere pairs that could be tracked through the sequence for at least 5 min (60 frames). Image stacks were then imported into UTHSCSA Image Tool for Windows Version 2.00 (University of Texas, Austin, TX) for frame-by-frame analysis. The  $x$ - $y$  position assigned to a centromere was determined by the brightest pixel at the center of the fluorescent signal and recorded on a spreadsheet (Microsoft Excel; Microsoft Corp., Redmond, WA). The distance between centromeres of a pair was calculated by triangulation. Three independent determinations were made of the position of each centromere in each frame of the movie and averaged. The series of separation distances was used to determine rates and durations of separation and coming together (relaxing) and the frequencies of transition between stretching and relaxing.

**Criteria for Selection of Centromere Pairs for Measurement of Dynamics.** Taxol® induced several spindle abnormalities, including lagging (uncongressed) chromosomes and multipolar spindles. For determination of centromere dynamics, only cells in which the majority of chromosomes had congressed to a well-formed and distinct metaphase plate were used, and only centromere pairs of congressed chromosomes were analyzed. Preliminary comparison of tripolar spindles and bipolar spindles indicated that the dynamics of centromeres in tripolar spindles were somewhat greater than in bipolar spindles. For this reason, we included only bipolar spindles for measurement at 10–50 nM Taxol®. However, bipolar spindles were relatively difficult to

find at higher Taxol® concentrations; thus, at 100 nM Taxol®, all spindles were included in the reported measurements (7 pairs from 2 bipolar spindles and 13 pairs from 9 tripolar spindles). Suppression of centromere dynamics in all spindles was virtually complete at 100 nM Taxol®, and because the inclusion of tripolar spindles would only increase the measured dynamics, their inclusion did not affect the conclusions drawn.

**Determination of Background Movement.** To determine how much of the observed centromere movement was attributable to simple diffusion or to electronic noise rather than to microtubule dynamics and/or motor proteins, we measured centromere movements in the absence of microtubules. U2OS cells were incubated with 1  $\mu\text{M}$  vinblastine for 6 h, which completely depolymerized all of the microtubules (data not shown). The mean center-to-center separation between sister centromeres (seven pairs in three cells) in the absence of microtubules was  $0.66 \pm 0.03 \mu\text{m}$ , and the average rates of increasing and decreasing separation were  $0.55 \pm 0.03$  and  $0.58 \pm 0.03 \mu\text{m}/\text{min}$ , respectively. We then determined the total distance that a centromere moved toward and away from its sister for each interval of 5 s, 10 s, 15 s, . . . 300 s (the sum of all stretching and relaxing distances for each interval). These distances were averaged for all seven pairs of centromeres. The mean distance moved plotted against the length of interval was linear, with a slope of  $0.42 \mu\text{m}/\text{min}$  ( $r = 0.999$ ). Thus, we concluded that  $0.42 \mu\text{m}/\text{min}$  is the mean rate of movement in the absence of microtubules. Any movement less than this was considered to be background or diffusional movement and was classified as a “pause” or a movement that was so attenuated that it could not be reliably measured. We note that a slightly different value was used in (33) for determination of a “pause,” which resulted in different values for the control parameter.

## RESULTS

### Effects of Taxol® on Proliferation and Mitosis in U2OS Cells.

The goal of these experiments was to analyze centromere dynamics in living U2OS tumor cells at the lowest Taxol® concentrations that significantly inhibited proliferation and slowed or blocked mitosis. Thus, we first needed to determine the effects of Taxol® on proliferation, mitotic progression, and spindle microtubule organization in the cells. Cells were incubated with Taxol® (5–300 nM), and the increase in the number of live cells after 28 h (one cell cycle) was compared with the increase in the absence of Taxol®. As shown in Fig. 1 (○), proliferation was inhibited by 50% at 9 nM Taxol® and by 100% at 50 nM Taxol®.

The effects of Taxol® on mitosis were measured by determining the mitotic index and the ratio of cells in anaphase to cells in metaphase. As shown in Fig. 1 (□), at Taxol® concentrations greater

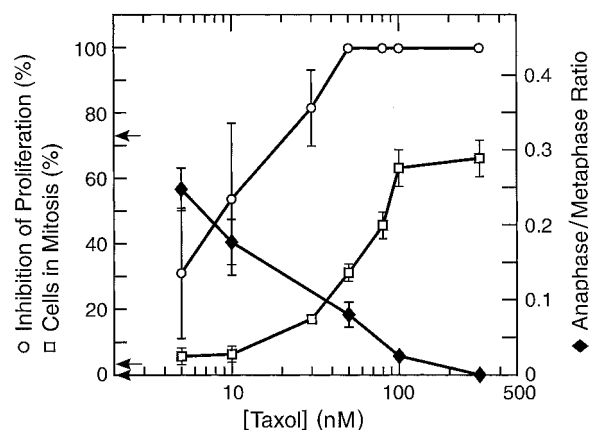


Fig. 1. Inhibition of proliferation of U2OS human osteosarcoma cells (○), accumulation of cells in mitosis (□), and inhibition of the cell cycle transition from metaphase to anaphase (◆) by Taxol® (28 h). Cell proliferation was determined by counting live cells at the time of Taxol® addition and 28 h later. Accumulation in mitosis and the ratio of cells in anaphase to cells in metaphase were determined by counting cells by immunofluorescence microscopy after fixation and staining of microtubules and chromatin. Values are the mean  $\pm$  SEs for three independent experiments.

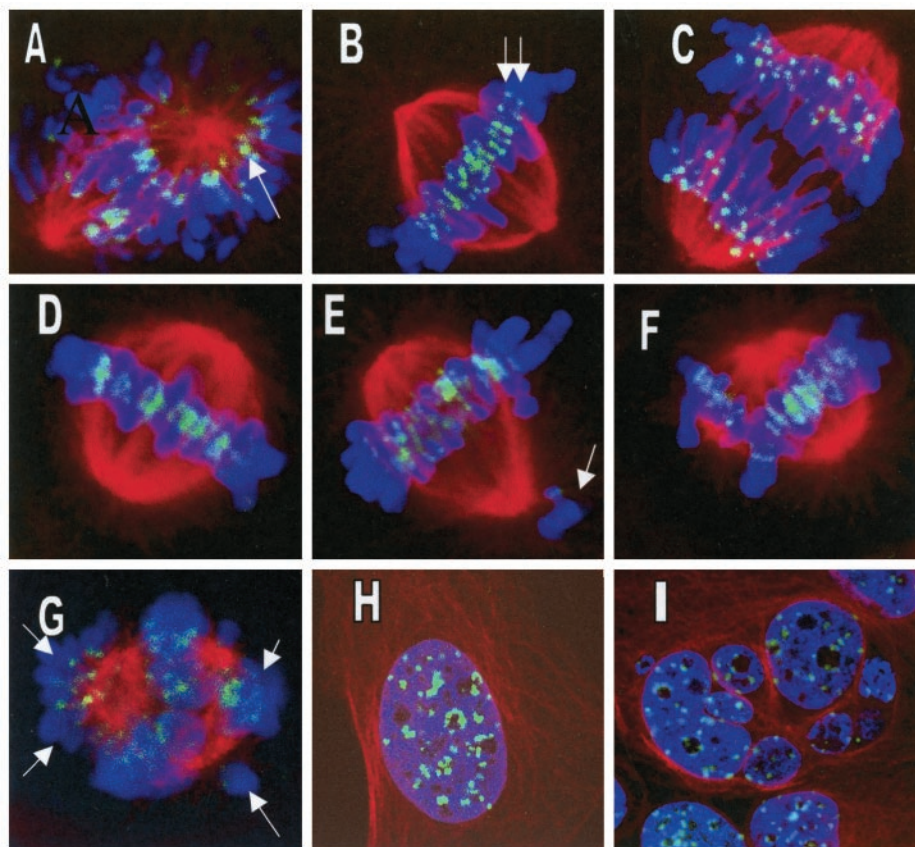


Fig. 2. Centromeres, microtubules, and chromosomes in U2OS cells in the absence (A–C and H) or presence (D–G and I) of Taxol®. Cells expressing GFP-CENP-B were incubated with Taxol® (28 h) or without Taxol®, fixed, stained with antibodies to  $\alpha$ -tubulin (red) and to histone protein (blue), and imaged by confocal microscopy. In control cells in prometaphase (A) and metaphase (B), pairs of sister centromeres are present on sister chromatids and are separated by variable distances (arrows). In anaphase (C), sister chromatids and centromeres have separated. In the presence of 10 nM Taxol® (D–F), some spindles appear normal and are bipolar with all chromosomes congressed to the metaphase plate (D), some have a few or many chromosomes that have not congressed and remain at one of the poles (arrow in E), and some are tripolar with three plates of congressed chromosomes (F). At 1  $\mu$ M Taxol® (G), spindle abnormalities are more severe, and many chromosomes have not congressed to the metaphase plate (arrows). In control cells in interphase (H), most cells have a single nucleus and a fine, well-spread array of microtubules, whereas in the presence of 10 nM Taxol® (I), many cells have multiple nuclei, and microtubules show a tendency toward side-by-side association.

than 10 nM, cells accumulated in mitosis, reaching a maximum of  $66.0 \pm 3.2\%$  at 300 nM Taxol® (28 h). To determine whether mitosis was only slowed or whether it was blocked at a particular stage of mitosis, we determined the ratio of cells in anaphase (with segregated chromosomes) to those in metaphase [with unsegregated chromosomes (Fig. 1,  $\blacklozenge$ )]. In control cells, the ratio was 0.31, and at 5 nM Taxol®, the ratio decreased to 0.25, indicating a slight inhibition of progress into anaphase. Transition into anaphase was inhibited by 50% at 12 nM Taxol® and by 90% at 100 nM Taxol®. These results indicate that the primary effects of Taxol® on mitosis in the U2OS cells occurred between 5 and 100 nM Taxol®, and thus we examined centromere dynamics in this Taxol® concentration range.

**Spindle and Microtubule Organization and Localization of GFP-CENP-B.** The localization of GFP-CENP-B, microtubules, and chromosomes in fixed and stained U2OS cells in the absence and presence of Taxol® (28-h incubation) is shown in Fig. 2. In control cells in prometaphase, chromosomes were dispersed throughout the forming bipolar spindle (Fig. 2A). GFP-CENP-B appeared as round, paired, fluorescent dots (arrows in Fig. 2, A and B) on the chromosomes, with varying separation between the members of a pair, and with varying degrees of alignment with respect to the axis of the forming spindle. At metaphase (Fig. 2B), all of the chromosomes were congressed at the metaphase plate, and the centromere pairs were oriented parallel to the spindle axis. The GFP-labeled centromeres appeared as either round or elongated spots ( $\sim 400$ – $650$  nm diameter). During anaphase, sister chromatids and their associated centromeres became physically separated, and their centromeres appeared as single, spherical dots (Fig. 2C). After incubation for 28 h in 10 nM Taxol®, some spindles appeared normal and bipolar with all chromosomes congressed to the metaphase plate (Fig. 2D), whereas others had one or more chromosomes that remained uncongressed and were

located at one or both spindle poles (Fig. 2E, arrow). Most of the spindles ( $70.3 \pm 4.7\%$ ) were tripolar or multipolar (Fig. 2F; Table 1). GFP-centromere pairs were similar in appearance to those in control cells. At higher Taxol® concentrations (50 nM to 1  $\mu$ M), all spindles were abnormally organized with many uncongressed chromosomes (Fig. 2G, arrows) and with tripolar spindles predominating ( $>90\%$ ). Interphase microtubules were generally single and well-dispersed at 10–50 nM (Fig. 2I), but distinct bundles of microtubules formed at 100 nM Taxol® (data not shown).

**Dynamic Behavior of Centromeres in Living Cells.** Sister centromeres, as observed by confocal microscopy in living mitotic cells, alternated between phases of increasing and decreasing separation; they stretched apart and then relaxed back together (20). The change in separation distance of a typical pair of centromeres over a period of 90 s in a control cell is shown in Fig. 3. In the first panel, at time 0, the sister centromeres were separated by  $0.9 \mu\text{m}$ , in the second panel (55 s), they were separated by  $1.4 \mu\text{m}$ , and in the third panel (90 s), they relaxed back together and were only  $0.7 \mu\text{m}$  apart.

Table 1 Spindle and nuclear abnormalities induced by Taxol® in U2OS cells

U2OS cells were incubated with Taxol® for 6 or 28 h. After fixation and staining for microtubules and chromatin (see “Materials and Methods”), the numbers of mitotic cells with multipolar, bipolar, or monopolar spindles as well as the number of interphase cells with multiple or single nuclei were counted by immunofluorescence microscopy. Values are the mean  $\pm$  SE of two experiments and represent counts from 100 to  $>500$  cells per concentration and time.

Taxol® concentration (nM)	Multipolar spindles, 6-h incubation (%)	Multinucleate interphase cells, 6-h incubation (%)	Multinucleate interphase cells, 28-h incubation (%)
0 (control)	$1.9 \pm 1.98$	$0.8 \pm 0.8$	$1.9 \pm 0.9$
10	$70.3 \pm 4.7$	$3.6 \pm 3.6$	$61.9 \pm 1.2$
50	$91.2 \pm 3.1$	$9.4 \pm 5.1$	$94.1 \pm 0.3$
100	$91.3 \pm 1.3$	$7.7 \pm 0.5$	96.1



Fig. 3. Dynamic behavior of centromeres in living U2OS cells in the absence of drug. Images of GFP-centromeres were collected from a single plane by confocal microscopy at 5-s intervals. Arrowheads indicate the positions of sister centromeres at time 0 (0.9  $\mu\text{m}$  separation), 55 s later (when they are maximally stretched apart to a distance of 1.4  $\mu\text{m}$ ), and at 90 s [when they have relaxed back together (0.7  $\mu\text{m}$  separation)].

Fig. 4 shows a time course for stretching and relaxing of two pairs of sister centromeres as determined from images like those shown in Fig. 3. The *top trace* is the distance in micrometers between the two members of a centromere pair in a control cell, and the *bottom trace* is the distance between the two members of a pair in the presence of 100 nM Taxol®. Such graphs are similar to “life history” plots of microtubule dynamics (for example, see Ref. 17). The rate, duration, and extent of each stretching or relaxing episode were determined from such graphs (“Materials and Methods”). For the centromere pair shown in the *top trace* in Fig. 4 (in the absence of Taxol®), the pair was separated by 0.8  $\mu\text{m}$  at time 0. At 40 s, the pair was separated by 1  $\mu\text{m}$  (the maximum separation observed for this pair), and 10 s later, the separation was 0.7  $\mu\text{m}$ . For some periods of time, ranging from 5 to 60 s, pairs often displayed little or no detectable change in separation distance, a phase that we called a pause [defined as movement that is not significantly different from background, (diffusional movement, which was determined to be 0.42  $\mu\text{m}/\text{min}$ ; see “Materials and Methods”). We also determined the frequency of transitions between phases of stretching and relaxing. The members of the lower centromere pair (100 nM Taxol®) were closer together than they were in the absence of Taxol®, and both the mean frequency and the mean amplitude of their movements relative to each other were reduced as compared with those of control centromeres.

**Centromere Dynamics in Control U2OS Cells.** The various centromere dynamics parameters we measured are shown in Tables 2 and 3 and Figs. 5 and 6. In the absence of Taxol®, centromere pairs in cells stretched and relaxed at similar rates and for similar durations of time. They stretched at a rate of  $0.76 \pm 0.04 \mu\text{m}/\text{min}$  for a duration of  $13.8 \pm 0.8 \text{ s}$  and relaxed at a rate of  $0.71 \pm 0.03 \mu\text{m}/\text{min}$  for a duration of  $16.6 \pm 1.2 \text{ s}$  (Table 2; Fig. 5). The mean separation distance was  $0.73 \pm 0.03 \mu\text{m}$  and ranged from a maximum of  $0.89 \pm 0.04 \mu\text{m}$  to a minimum of  $0.59 \pm 0.02 \mu\text{m}$ . Centromere pairs transitioned from a stretching phase to a pause or relaxing phase and from a relaxing phase to a pause or stretching phase at a frequency of  $0.81 \pm 0.14 \text{ transitions}/\text{min}$  (in other words, once every 74 s). Centromere pairs in control cells spent  $15.4 \pm 2.3\%$  of the time stretching,  $19.3 \pm 2.6\%$  of the time relaxing, and  $65.4 \pm 3.8\%$  of the time in a paused state. Here we use the term centromere “dynamicity” in a manner analogous to its use in describing microtubule dynamics (22), the sum of the all of the stretching and relaxing distances divided by the total time observed. The mean centromere dynamicity in control cells was 0.25  $\mu\text{m}/\text{min}$ .

**Taxol® Significantly Suppressed Centromere Dynamics.** We note that at the lowest Taxol® concentration examined (10 nM), the mean values of several centromere dynamics parameters increased slightly (Tables 2 and 3; Fig. 6), but none of the increases was significant at the 90% confidence level (Student’s *t* test). The most prominent changes in centromere dynamics at 50 and 100 nM Taxol® were reductions in the transition frequency, the dynamicity, and the separation distance between sister centromeres and an increase in the pause time. For example, 50 nM Taxol® reduced the transition frequency by 27% from  $0.81 \pm 0.14$  to  $0.59 \pm 0.07 \text{ events}/\text{min}$ . It also reduced the dynamicity by 24% and reduced the mean maximal and

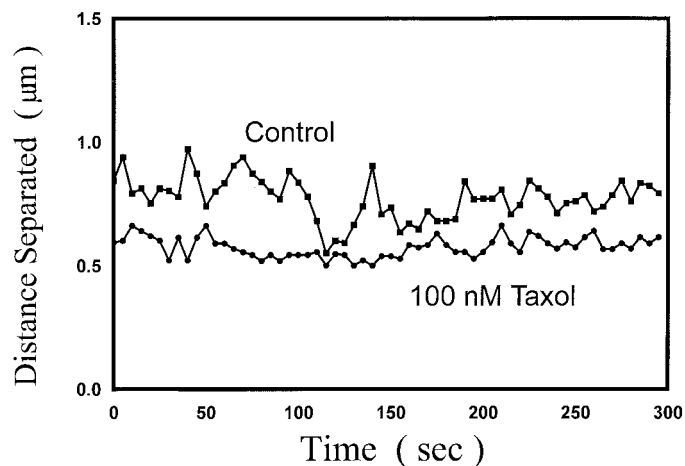


Fig. 4. Time course of changes in the center-to-center separation distance between a pair of sister centromeres in the absence of Taxol® (*top trace*) and in the presence of 100 nM Taxol® (*bottom trace*). Images of GFP-centromeres were collected from a single plane by confocal microscopy at 5-s intervals. Separation distances between the two members of pairs that remained well-focused for the 5-min recording period were measured as described in “Materials and Methods.” The separation between the members of a pair alternated between episodes of stretching and episodes of relaxing. For example, at time 0, in the absence of Taxol®, the pair was separated by 0.8  $\mu\text{m}$ . At 40 s, the pair was separated by 1  $\mu\text{m}$  (the maximum separation observed for this pair), and 10 s later, the separation was reduced to 0.7  $\mu\text{m}$ . The minimum separation observed for this pair was 0.5  $\mu\text{m}$  and occurred at 120 s. The characterization of events on the upper trace as stretching (increasing separation, I), decreasing separation or relaxing (R), or pause (P) was as follows: P, 0–40 s; R, 40–50 s; I, 50–70 s; R, 70–90 s; P, 90–95 s; R, 95–115 s; I, 115–140 s; P, 155–215 s; I, 215–225 s; R, 225–240 s; and P, 240–300 s. In the presence of 100 nM Taxol®, the separation distance was reduced overall and ranged from 0.50 to 0.66  $\mu\text{m}$  in this trace. The characterization of events on the lower trace was as follows: P, 0–35 s; I, 35–45 s; P, 45–195 s; I, 195–210 s; and P, 210–300 s.

Table 2 *Centromere dynamics parameters*

Between 14 and 30 pairs of centromeres from between 7 and 11 cells were measured for each condition.

Parameter	Control	10 nM Taxol®		50 nM Taxol®		100 nM Taxol®	
Rate of stretching ( $\mu\text{m}/\text{min}$ )	$0.76 \pm 0.04$	$0.80 \pm 0.03$	+10%	$0.77 \pm 0.04$	+6%	$0.62 \pm 0.02^a$	-15%
Rate of relaxing ( $\mu\text{m}/\text{min}$ )	$0.71 \pm 0.04$	$0.78 \pm 0.04$	+10%	$0.69 \pm 0.02$	-3%	$0.58 \pm 0.02^a$	-18%
Duration of stretching (s)	$13.8 \pm 0.8$	$16.3 \pm 1.6$	+18%	$13.0 \pm 0.5$	-6%	$11.6 \pm 0.5^a$	-16%
Duration of relaxing (s)	$16.6 \pm 1.2$	$15.1 \pm 1.2$	-9%	$13.9 \pm 0.5$	-16%	$11.6 \pm 0.5^a$	-30%
Transition frequency (events/min)	$0.81 \pm 0.14$	$1.00 \pm 0.11$	+24%	$0.59 \pm 0.07$	-27%	$0.53 \pm 0.08^b$	-35%
Centromere dynamicity ( $\mu\text{m}/\text{min}$ )	0.25	0.33	+32%	0.19	-24%	0.11	-56%

<sup>a</sup> Values were significantly different from control values at the 98% confidence level (Student's *t* test).<sup>b</sup> Values were significantly different from control values at the 90% confidence level (Student's *t* test).

minimal separation distances between centromeres (by 11% and 14%, respectively). Finally, it increased the percentage of time paused by 14%.

At 100 nM Taxol®, in addition to affecting the same parameters discussed above for 50 nM Taxol®, both the rates and durations of stretching and relaxation were also suppressed (Table 2; Fig. 5). For example, the rates of separation and relaxation were decreased by 15% and 18%, respectively. The durations of separation and relaxation also decreased, by 16% and 30%, respectively. There was also a large (56%) decrease in dynamicity at 100 nM Taxol® [from 0.25  $\mu\text{m}/\text{min}$  in controls to 0.11  $\mu\text{m}/\text{min}$  in 100 nM Taxol® (Table 2; Fig. 6D)]. Thus, as shown pictorially in Fig. 5, centromeres did not stretch apart as fast or as far or for as long or as frequently as they did in control cells. They also did not relax together as fast, as long, or as frequently as they did in control cells. Taken together, these results indicate that the movements of the centromeres were suppressed in a concentration-dependent manner by Taxol®. These results are consistent with a mechanism in which microtubule dynamics play a major role in centromere dynamics.

#### Abnormal Mitoses Resulted in Multinucleate Interphase Cells.

Mitotic spindle abnormalities developed rapidly after addition of Taxol®, but abnormalities in interphase cells were detectable only after many hours of incubation with Taxol® and appeared to result from earlier mitotic block. After 6 h of incubation with Taxol®, most interphase cells appeared normal and had a single nucleus (>90%), similar to control cells (99.3% mononucleate; Table 1). However, after 28 h of incubation with 10 nM Taxol®, 61.9  $\pm$  1.2% of interphase cells were multinucleate (compare control in Fig. 2H with Fig. 2I, 10 nM), and >94% were multinucleate at 50–100 nM Taxol® (Table 1). Thus, although many blocked cells eventually exited mitosis, cytokinesis was unsuccessful, multinucleate cells formed, and proliferation was inhibited (Fig. 1).

## DISCUSSION

Using GFP-CENP-B as a marker for centromeres, kinetochores, and the plus ends of kinetochore microtubules, we have analyzed the effects of Taxol on centromere dynamics in living U2OS cells. We found that 50–100 nM Taxol® significantly suppressed the stretching and relaxing dynamics of centromeres on sister chromatids. The time that centromeres were in a paused state increased, and the separation distance between sister centromeres and the frequency of transitions

between stretching and relaxing decreased. Taxol® (50 nM) reduced the centromere dynamicity by 24%, and 100 nM Taxol® reduced it by 55%. These effects on centromere/kinetochore dynamics were associated with maximal mitotic accumulation (63%), a >90% block of the metaphase/anaphase transition, and complete inhibition of proliferation.

**Centromere Dynamics in the Absence of Taxol®.** The movements of sister centromeres in control cells were characterized by periodic transitions from stretching apart to relaxing back together. On average, a centromere pair transitioned 1.2 times/min from stretching to relaxing and *vice versa*. Each kinetochore and its adjacent centromere is the site of attachment of 20–30 individual microtubules (23, 24). When the centromeres are stretching, the attached microtubules on the sister kinetochores must be shortening. When the centromeres are relaxing, the attached microtubules must be growing. The transitions between centromere stretching and relaxation were abrupt and must represent simultaneous and tightly coordinated phases of growth and shortening of all of the microtubules attached to an individual kinetochore/centromere.

**The Kinetochore-dependent Spindle Checkpoint, Intercentromere Distance, and the Maintenance of Spindle Tension.** The kinetochore-dependent spindle checkpoint delays anaphase onset until all chromosomes have properly attached to the spindle microtubules and become aligned at the metaphase plate (25). Passage through the checkpoint depends upon tension generated at kinetochores, upon occupancy of kinetochores by a sufficient number of dynamic microtubules, or both (26). For example, the checkpoint block induced by a chromosome that remains unattached to the spindle can be relieved by applying tension mechanically to its kinetochore. As kinetochore-attached microtubules grow in length, the intercentromere distance shortens, and tension on the kinetochores is diminished. As the attached microtubules shorten, the intercentromere distance lengthens, and thus tension on the kinetochores increases. Taxol® (50–100 nM) reduced the mean intercentromere separation distance by 11% (Table 3), diminishing tension on kinetochores and thus invoking the kinetochore-dependent spindle checkpoint.

We note that our results suggest that individual centromere pairs in control cells are not always under tension. The mean minimal separation of sister centromeres in the absence of Taxol® was 0.59  $\mu\text{m}$ , a value similar to the mean centromere separation after depolymerization of all microtubules with 1  $\mu\text{M}$  vinblastine (0.66  $\mu\text{m}$ ). This

Table 3 *Centromere dynamics parameters*

Parameter	Control	10 nM Taxol®		50 nM Taxol®		100 nM Taxol®	
Time stretching (%)	$15.4 \pm 2.3$	$20.5 \pm 2.6$	+33%	$11.6 \pm 1.1$	-25%	$10.1 \pm 1.3$	-34%
Time relaxing (%)	$19.3 \pm 2.6$	$21.2 \pm 2.8$	+10%	$14.0 \pm 1.7$	-28%	$8.9 \pm 1.2$	-54%
Time paused (%)	$65.4 \pm 3.8$	$58.4 \pm 4.2$	-11%	$74.4 \pm 2.5^b$	+14%	$81.0 \pm 1.8^d$	+24%
Mean separation ( $\mu\text{m}$ )	$0.73 \pm 0.03$	$0.73 \pm 0.03$	0%	$0.65 \pm 0.01^c$	-11%	$0.65 \pm 0.02^c$	-11%
Mean maximal separation ( $\mu\text{m}$ ) <sup>a</sup>	$0.89 \pm 0.04$	$0.93 \pm 0.04$	+5%	$0.79 \pm 0.01^d$	-11%	$0.76 \pm 0.01^d$	-15%
Mean minimal separation ( $\mu\text{m}$ ) <sup>a</sup>	$0.59 \pm 0.02$	$0.56 \pm 0.02$	-5%	$0.51 \pm 0.01^d$	-14%	$0.54 \pm 0.01$	-9%

<sup>a</sup> The mean for all tracings of the two maximal separations (peaks) or the two minimal separations (valleys) during each 5-min tracing for each condition.<sup>b,c,d</sup> Values were significantly different from control values at the 90%, 95%, or 98% confidence level, respectively (student's *t* test).

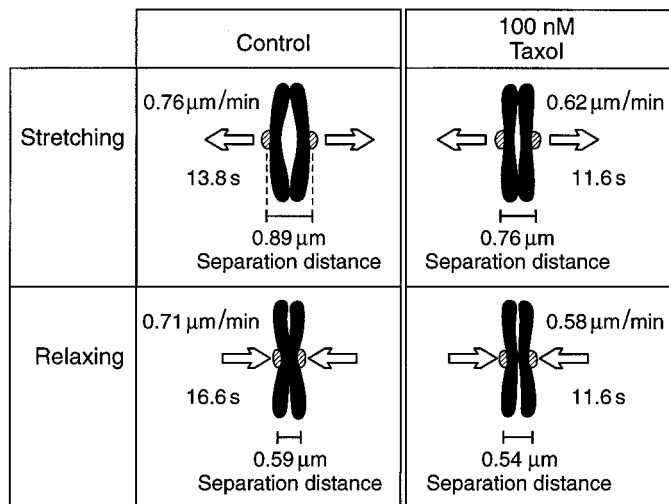


Fig. 5. Diagram illustrating the effects of Taxol® on centromere and microtubule dynamics. The *left panels* illustrate a pair of sister chromatids and their centromeres/kinetochores in the absence of Taxol®, whereas the *right panels* illustrate a pair of chromatids in the presence of 100 nM Taxol®. The rates and durations of centromere stretching (*top panels*) and relaxation (*bottom panels*) and the mean maximal and minimal separation distances are indicated.

indicates that during normal fluctuations of centromere stretching and relaxation, the individual centromere pairs transiently relax to a state in which no tension is apparent. However, the overall mean separation distance in the absence of drugs was 0.73  $\mu\text{m}$ , indicating that, on average, centromeres attached to the spindle are under tension.

It is conceivable that when the centromeres are completely relaxed and there is no tension, this state may signal or facilitate the simultaneous transition of all of the attached microtubules to switch from a growing state to a shortening state, which then recreates increased tension. The gain and loss of a stabilizing GTP-tubulin or GDP-Pi-tubulin cap are thought to regulate the growing and shortening transitions associated with microtubule dynamic instability (27, 28). When microtubules are capped by GTP/GDP-Pi they grow, and when the cap is lost, the end contains only GDP-tubulin, and the microtubule shortens rapidly. One possibility is that transition between centromere relaxation and stretching could be due to the loss of the GTP-tubulin cap at the ends of the growing microtubules when they are compressed and no longer under tension. Thus, the complete loss of tension at the centromeres may signal the uncapping of microtubule ends and thus coordinate the synchronized depolymerization of all of the microtubules in the microtubule bundle attached to a kinetochore, thus leading to a transition to stretching. The tension that develops as the degree of stretching increases may then facilitate reformation of the stabilizing cap at the microtubule ends and transition back to microtubule growth, leading in turn to centromere relaxation. In support of this model, the association and dissociation rate constants for tubulin at the microtubule ends can be altered by compression resulting from the growing end of a microtubule hitting the "wall" represented by the centromere mass, thus leading to GTP-cap loss (29, 30). It is also conceivable that conformational changes in tubulin as a result of increased tension on the microtubule lattice during stretching may enhance the capping reaction, leading to synchronized microtubule regrowth and thus to a transition from stretching to relaxation.

**Microtubule Dynamics, Rather Than Microtubule Motors, May Be Primarily Responsible for Centromere Stretching and Relaxation.** The rates of centromere separation and relaxation in control cells ( $\sim 0.7 \mu\text{m}/\text{min}$ ) are relatively slow as compared with the rates of growth and shortening of individual microtubules measured in living cells. For example, the rates of microtubule growth and short-

ening during interphase in A498 human kidney and CaOv-3 ovarian carcinoma cells are 10–17-fold faster (17) than the rates of centromere stretching and relaxation reported here. In addition, the dynamicity of microtubules in mitotic asters is severalfold higher than that for interphase microtubules (31, 32). Centromere dynamics may be slowed to rates that are significantly slower than the inherent growth and shortening rates of individual microtubules by the arrangement of microtubules at the centromere/kinetochore. Bundles of microtubules from opposite spindle poles are attached to sister kinetochores. Individual microtubules in each bundle may not be perfectly synchronous in their transitions between growth and shortening and thus may work against each another. In addition, centromere dynamics are the result of competing growing and shortening of the opposing microtubule bundles, and thus the net rates may be suppressed by the competition between them. Although other possibilities exist, the slow rates of centromere stretching/relaxation movements indicate that centromere dynamics could be accounted for primarily by microtubule dynamics and may not require significant energetic contributions from microtubule motors. This suggestion is strengthened by the observation that two very different drugs, vinblastine and Taxol®, both suppress centromere dynamics (33) and reduce the intercentromere distance (20, 34). Vinblastine is a microtubule-binding drug that suppresses microtubule dynamics by binding with high affinity to the ends of microtubules rather than to their interior surfaces as Taxol® does (35–37). Given the different binding sites for Taxol® and vinblastine

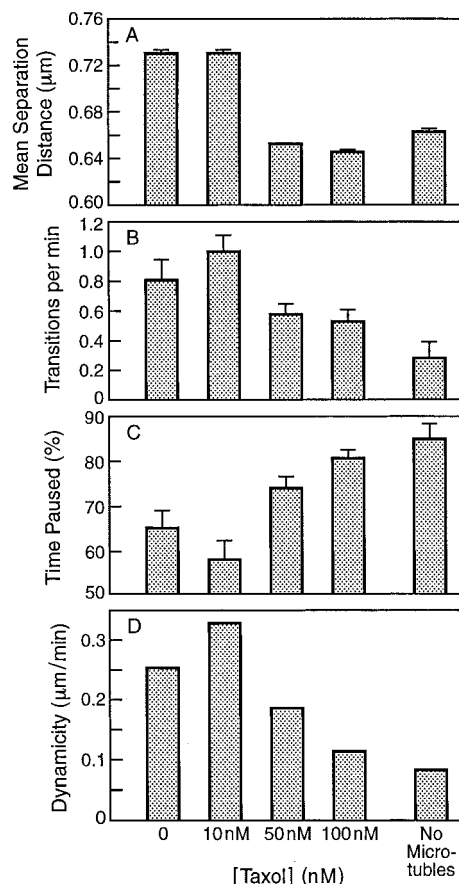


Fig. 6. Histograms illustrating the effects of Taxol® (10–100 nM) on centromere dynamics in living U2OS cells. *A*, average sister centromere separation. *B*, frequency of transition from stretching to relaxation and *vice versa*. *C*, percentage of time in a state of pause when sister centromeres were neither separating nor relaxing detectably. *D*, the rate of dynamicity or overall dynamics. In each panel, the *right-hand bar* indicates the value of the parameter in the absence of microtubules, as induced by incubation of the cells with 1  $\mu\text{M}$  vinblastine for 6 h.

on microtubules, it is unlikely that both Taxol® and vinblastine suppress centromere dynamics by sterically blocking the interaction of motor proteins with microtubules. Rather, their suppression of centromere dynamics can be most readily attributed to their common suppression of microtubule dynamics. Thus, during metaphase, microtubule motor proteins may serve primarily to attach kinetochores to the dynamic microtubules or to directly modulate microtubule dynamics (38) rather than to act in a motoring capacity.

Low concentrations of Taxol® (10 nM) may induce slightly increased centromere dynamics in cells, whereas high Taxol® concentrations (50–100 nM) suppress dynamics. We found that 10 nM Taxol® slightly increased the rate and duration of stretching, the rate of relaxing, the transition frequency, the total time spent separating and relaxing, and the centromere dynamicity. Although none of these effects was statistically significant by itself, the combination of all of the changes in these parameters in the direction of increased centromere dynamics suggests that an interesting interaction may occur between partially stabilized microtubule ends and their attached kinetochores. It is possible that a microtubule motor protein might act more efficiently on a partially stabilized microtubule end than on a very labile microtubule end and thus bring about slightly increased centromere dynamics at low Taxol® concentrations. The increased dynamics may induce an increase in tension on kinetochores, resulting in premature anaphase chromosome segregation and aneuploidy. At higher Taxol® concentrations, kinetochore movement involving any motor action might be impeded altogether by the more stabilized microtubule end.

**The Mitotic Checkpoint Is Sensitive to Slight Suppression of Microtubule Dynamics.** In living U2OS cells, it appears that minimal suppression of microtubule dynamics can significantly suppress centromere dynamics, reducing tension on the kinetochores/centromeres to zero, invoking the spindle checkpoint, and inhibiting progression into anaphase. A 15% and 18% reduction in the rates of stretching and relaxation, respectively, and a 16% and 30% reduction in the durations of stretching and relaxation, respectively (at 100 nM Taxol®), are sufficient to nearly completely inhibit the transition from metaphase into anaphase.

**The Relationship between Mitotic Block and Inhibition of Proliferation by Taxol®.** At low Taxol® concentrations, *e.g.*, 5–10 nM, the mitotic index increased slightly (from 1.3% to 4.2%; Fig. 1), progress from metaphase to anaphase was slowed but not blocked, and proliferation was inhibited by 31% (Fig. 1). Thus, interestingly, at low Taxol® concentrations, mitosis was not blocked, even though cell proliferation was significantly inhibited. At low Taxol® concentrations, microtubules appear to be sufficiently dynamic that the mitotic checkpoint is eventually satisfied, and anaphase ensues. Thus, at low concentrations, Taxol® appears to inhibit cell proliferation not by a long-term block of mitosis but by another mechanism. This mechanism may involve the production of multipolar spindles (Table 1), which ultimately induces abnormal chromosome segregation and aborted cytokinesis. In some cells lines, anaphase in the presence of low concentrations of Taxol® (< 10 nM) results in abnormal chromosome segregation, abnormal DNA content and cell size, aneuploidy, and cell death (39, 40).<sup>4</sup>

**Summary.** High concentrations of Taxol® (100 nM) significantly suppressed centromere dynamics and were associated with maximal mitotic accumulation (63%), > 90% block of the metaphase/anaphase transition, and complete inhibition of proliferation. Intercentromere distances were minimal; they were equivalent to the separations observed in the absence of attached microtubules. Thus, the tension on

the centromeres in the presence of Taxol® was virtually nonexistent. These results are a direct demonstration that dynamic microtubules are necessary for the transition from metaphase to anaphase. The strict Taxol® concentration dependence between the degree of suppression of kinetochore microtubule dynamics and the degree of mitotic block strongly indicates that the primary mechanism of mitotic block by Taxol® is suppression of microtubule dynamics of kinetochore microtubules.

## ACKNOWLEDGMENTS

We thank Kathryn Kamath for critical reading of the manuscript.

## REFERENCES

- Rowinsky, E. The development and clinical utility of the taxane class of antimicrotubule chemotherapy agents. *Annu. Rev. Med.*, **48**: 353–374, 1997.
- Schiff, P. B., Fant, J., and Horwitz, S. B. Promotion of microtubule assembly *in vitro* by Taxol. *Nature (Lond.)*, **277**: 665–667, 1979.
- Kumar, N. Taxol-induces polymerization of purified tubulin. *J. Biol. Chem.*, **256**: 10435–10441, 1981.
- Howard, W. D., and Timasheff, S. N. Linkages between the effects of Taxol, colchicine, and GTP on tubulin polymerization. *J. Biol. Chem.*, **263**: 1342–1346, 1988.
- Jordan, M. A., Toso, R. J., Thrower, D., and Wilson, L. Mechanism of mitotic block and inhibition of cell proliferation by Taxol at low concentrations. *Proc. Natl. Acad. Sci. USA*, **90**: 9552–9556, 1993.
- Derry, W. B., Wilson, L., and Jordan, M. A. Substoichiometric binding of Taxol suppresses microtubule dynamics. *Biochemistry*, **34**: 2203–2211, 1995.
- Derry, W. B., Wilson, L., and Jordan, M. A. Low potency of Taxol at microtubule minus ends: implication for its anti-mitotic and therapeutic mechanism. *Cancer Res.*, **58**: 1177–1184, 1998.
- Rieder, C., Schultz, A., Cole, R., and Sluder, G. Anaphase onset in vertebrate somatic cells is controlled by a checkpoint that monitors sister kinetochore attachment to the spindle. *J. Cell Biol.*, **127**: 1301–1310, 1994.
- Milas, L., Hunter, N. R., Kurdoglu, B., Mason, K. A., Meyn, R., Stephens, L. C., and Peters, L. J. Kinetics of mitotic arrest and apoptosis in murine mammary and ovarian tumors treated with Taxol. *Cancer Chemother. Pharmacol.*, **35**: 297–303, 1995.
- Jordan, M. A., Wendell, K. L., Gardiner, S., Derry, W. B., Copp, H., and Wilson, L. Mitotic block induced in HeLa cells by low concentrations of paclitaxel (Taxol) results in abnormal mitotic exit and apoptotic cell death. *Cancer Res.*, **56**: 816–825, 1996.
- Mitchison, T. J., and Kirschner, M. Dynamic instability of microtubule growth. *Nature (Lond.)*, **312**: 237–242, 1984.
- Margolis, R. L., and Wilson, L. Opposite end assembly and disassembly of microtubules at steady state *in vitro*. *Cell*, **13**: 1–8, 1978.
- Rodionov, V. I., and Borisy, G. G. Microtubule treadmilling *in vivo*. *Science (Wash. DC)*, **275**: 215–218, 1997.
- Mitchison, T. J. Poleward microtubule flux in the mitotic spindle; evidence from photoactivation of fluorescence. *J. Cell Biol.*, **109**: 637–652, 1989.
- Hayden, J. J., Bowser, S. S., and Rieder, C. Kinetochores capture astral microtubules during chromosome attachment to the mitotic spindle: direct visualization in live newt cells. *J. Cell Biol.*, **111**: 1039–1045, 1990.
- Waterman-Storer, C., and Salmon, E. D. Microtubule dynamics: treadmilling comes around again. *Curr. Biol.*, **7**: 369–372, 1997.
- Yvon, A.-M., Wadsworth, P., and Jordan, M. A. Taxol suppresses dynamics of individual microtubules in living human tumor cells. *Mol. Biol. Cell*, **10**: 947–949, 1999.
- Goncalves, A., Braguer, D., Kamath, K., Martello, L., Briand, C., Horwitz, S., Wilson, L., and Jordan, M. A. Resistance to Taxol in lung cancer cells associated with increased microtubule dynamics. *Proc. Natl. Acad. Sci. USA*, **98**: 11737–11741, 2001.
- Skibbens, R. V., Skeen, V. P., and Salmon, E. D. Directional instability of kinetochore motility during chromosome congression and segregation in mitotic newt lung cells: a push-pull mechanism. *J. Cell Biol.*, **122**: 859–875, 1993.
- Shelby, R. D., Hahn, K. M., and Sullivan, K. F. Dynamic elastic behavior of  $\alpha$ -satellite DNA domains visualized *in situ* in living human cells. *J. Cell Biol.*, **135**: 545–557, 1996.
- Jordan, M. A., and Wilson, L. The use and action of drugs in analyzing mitosis. *Methods Cell Biol.*, **61**: 267–295, 1999.
- Toso, R. J., Jordan, M. A., Farrell, K. W., Matsumoto, B., and Wilson, L. Kinetic stabilization of microtubule dynamic instability *in vitro* by vinblastine. *Biochemistry*, **32**: 1285–1293, 1993.
- Wendell, K. L., Wilson, L., and Jordan, M. A. Mitotic block in HeLa cells by vinblastine: ultrastructural changes in kinetochore-microtubule attachment and in centromeres. *J. Cell Sci.*, **104**: 261–274, 1993.
- McEwen, B., Heagle, A., Cassels, G., Buttle, K., and Rieder, C. Kinetochore fiber maturation in PtK1 cells and its implications for the mechanisms of chromosome congression and anaphase onset. *J. Cell Biol.*, **137**: 1567–1580, 1997.
- McIntosh, J., Grishchuk, E. L., and West, R. R. Chromosome-microtubule interactions during mitosis. *Annu. Rev. Cell Dev. Biol.*, **18**: 193–219, 2002.

<sup>4</sup> M. A. Jordan and L. Wilson, unpublished observations.

26. Nicklas, R. B., Waters, J. C., Salmon, E. D., and Ward, S. C. Checkpoint signals in grasshopper meiosis are sensitive to microtubule attachment, but tension is still essential. *J. Cell Sci.*, *114*: 4173–4183, 2001.
27. Carlier, M. F., and Pantaloni, D. Kinetic analysis of guanosine-5'-triphosphate hydrolysis associated with tubulin polymerisation. *Biochemistry*, *20*: 1918–1924, 1981.
28. Panda, D., Miller, H., and Wilson, L. Determination of the size and chemical nature of the stabilizing cap at microtubule ends using modulators of polymerization dynamics. *Biochemistry*, *41*: 1609–1617, 2002.
29. Hill, T. L. Theoretical problems related to the attachment of microtubules to kinetochores. *Proc. Natl. Acad. Sci. USA*, *82*: 4404–4408, 1985.
30. Hill, T. L., and Kirschner, M. W. Subunit treadmill of microtubules or actin in the presence of cellular barriers: possible conversion of chemical free energy into mechanical work. *Proc. Natl. Acad. Sci. USA*, *79*: 490–494, 1982.
31. Saxton, W. M., Stemple, D. L., Leslie, R. J., Salmon, E. D., Zavortnik, M., and McIntosh, J. R. Tubulin dynamics in cultured mammalian cells. *J. Cell Biol.*, *99*: 2175–2186, 1984.
32. Rusan, N. M., Fagerstrom, C. J., Yvon, A-M. C., and Wadsworth, P. Cell cycle-dependent changes in microtubule dynamics in living cells expressing green fluorescent protein- $\alpha$  tubulin. *Mol. Biol. Cell*, *12*: 971–980, 2001.
33. Okouneva, T., Hill, B. T., Wilson, L. and Jordan, M. A. The effects of vinflunine, vinorelbine, and vinblastine on centromere dynamics. *Mol. Cancer Ther.*, *2*, in press, 2003.
34. Skoufias, D. A., Andreassen, P., Lacroix, F., Wilson, L., and Margolis, R. L. Mammalian mad2 and bub1/bubR1 recognize distinct spindle-attachment and kinetochore-tension checkpoints. *Proc. Natl. Acad. Sci. USA*, *10*: 4492–4497, 2001.
35. Wilson, L., Jordan, M. A., Morse, A., and Margolis, R. L. Interaction of vinblastine with steady-state microtubules *in vitro*. *J. Mol. Biol.*, *159*: 129–149, 1982.
36. Jordan, M. A., Margolis, R. L., Himes, R. H., and Wilson, L. Identification of a distinct class of vinblastine binding sites on microtubules. *J. Mol. Biol.*, *187*: 61–73, 1986.
37. Nogales, E., Wolf, S. G., Khan, I. A., Luduena, R. F., and Downing, K. A. Structure of tubulin at 6.5 Å and location of the Taxol-binding site. *Nature (Lond.)*, *375*: 424–427, 1995.
38. Desai, A., Verma, S., Mitchison, T. J., and Walczak, C. E. Kin I kinesins are microtubule-destabilizing enzymes. *Cell*, *96*: 69–78, 1999.
39. Torres, K., and Horwitz, S. B. Mechanisms of Taxol-induced cell death are concentration dependent. *Cancer Res.*, *58*: 3620–3626, 1998.
40. Chen, J-G. and Horwitz, S. B. Differential mitotic responses to microtubule-stabilizing and -destabilizing drugs. *Cancer Res.*, *62*: 1935–1938, 2002.